Designing an Approach to Imaging MDSCs *in vivo*

A Technical Report submitted to the Department of Biomedical Engineering

Presented to the Faculty of the School of Engineering and Applied Science
University of Virginia • Charlottesville, Virginia

In Partial Fulfillment of the Requirements for the Degree
Bachelor of Science, School of Engineering

Sophia Kerns
Spring, 2022

On my honor as a University Student, I have neither given nor received unauthorized aid on this assignment as defined by the Honor Guidelines for Thesis-Related Assignments

Timothy Bullock, Department of Pathology
Richard Price, Department of Biomedical Engineering
Natasha Sheybani, Department of Biomedical Engineering

Designing an Approach to Fluorescently Imaging MDSCs *in vivo*

Sophia Kerns, Marissa Gonzalez, Lydia Petricca, Zehra Demir, Delaney Fisher, Tor Breza, Andrew Thim, Beata Chertok, Sara Kaswan, Natasha Sheybani, Richard Price, Timothy Bullock

Abstract

Myeloid Derived Suppressor Cells (MDSCs) are an extremely important immune cell subtype to study in the cancer immunology field, as they have been shown to be upregulated in certain tumor models and in focused ultrasound (FUS) experiments. These cells are characterized by Ly6G. Current methods of imaging these immune cells require that the organs and tumors be harvested, which does not allow observation of MDSC tumor infiltration at various treatment time points. Fluorescent imaging probes provide a way of imaging MDSC tumor infiltration at different time points throughout an experiment. Here, we aim to design a fluorescent imaging probe for *in vivo* use in mice through the use of antibodies conjugated to fluorophores. Preliminary experiments were completed to design the imaging probe as well as to determine a candidate cell line for *in vitro* testing of this probe. An *in vivo* pilot study was performed to both observe fluorophore efficacy and to observe the kinetics of the Ly6G antibody.

Keywords: Myeloid Derived Suppressor Cells, MDSC, Ly6G, fluorescent imaging

Introduction

Past studies in Focused Ultrasound (FUS) have shown elevated levels of myeloid derived suppressor cells (MDSCs) in the tumor microenvironment (TME). All MDSCs express CD11b[1]. MDSCs are classified as either granulocytic, marked by Ly6G, or monocytic, marked by Ly6C[2]. The focus of this project is imaging granulocytic MDSCs.

G-MDSCs have negative impacts on the immune system's response to tumors[3]. Granulocytic MDSCs specifically produce reactive oxygen species. T cells are suppressed by MDSCs, and regulatory T cells are upregulated[3]. MDSCs also crosstalk with other macrophages that suppress immune responses to cancer[4]. MDSC numbers also increase as cancer progresses, with later stages showing more MDSCs[3]. Other impacts of MDSCs include arginine and cysteine levels; reactive oxygen species upregulation; IL-10 and TGF-B production; increased PD-L1; reduced T cell receptor antigen recognition; and increased production of angiogenic factors[5]. MDSCs and the TME each impact each other to promote both tumor growth and MDSC proliferation[6,7]. These effects indicate that a greater understanding of MDSCs is warranted, especially in the context of FUS.

Imaging and counting immune cells can provide important information about how the immune system is responding to treatments. There are three main current approaches to this sort of data collection. The first is immunohistochemistry (IHC). This requires a tissue biopsy, fixing the tissue, and then staining for markers specific to the cells of interest[8]. A second approach is RNA-seq, which characterizes the RNA expression of the whole TME[9]. The third is tumor digestion and flow cytometry to count cells[10]. Each of these approaches provides information on either cell counts or cell location within specific organs. While IHC provides spatial and count information, it can only be done in slices of the tumor or organ rather than the whole mouse. Flow cytometry provides information about cell counts within the organ or tumor but does not provide information on

cell locations. Another issue with each of these things is that they require tumor removal in order to complete them, so they must be done at the final experimental time point.

Other approaches involve making probes to image the cells *in vivo. In vivo* imaging is helpful in that it can provide both spatial and cell count data on the cells of interest without having to euthanize a mouse. Specifically within the context of MDSCs, this is a helpful tool as it allows observation of how this cell population is changing over time and especially in response to treatments. *In vivo* imaging approaches either involve fluorescent imaging or radiolabeling. Radiolabeling involves conjugating a radioisotope to an antibody and is more commonly used than fluorescent imaging[7]. These are imaged using PET and MRI scans. Fluorescent imaging and radiolabeling are similar in that they both provide both spatial and cell count information. Although radiolabeling provides the ability to reconstruct tissue, fluorescent imaging can provide capabilities to better understand molecule location[11]. Fluorescent labeling has two main advantages over radiolabeling. The first is that it has a lower cost, which is advantageous for a probe that may be used frequently throughout treatments[12]. Another is that fluorescent probes have a much longer shelf life than radioisotopes, which means that they can be generated in larger batches that can be used repeatedly for more experimental consistency[12]. Due to these advantages, fluorescent imaging was chosen as the base for this study. Given the impacts that the TME can have on MDSCs and vice versa, the probe was also designed to infiltrate the tumor rather than attach to MDSC in circulation.

Antibodies provide a basis for targeting specific cells while allowing capability for conjugation to a fluorophore. These proteins can also be modified to better suit imaging applications. There are three main antibody fragments currently in use. These are the Fab, the scFv, and the VHH at 50, 28, and 15 kDa respectively. A molecular weight of less than 60 kDa is required for renal clearance, which allows a better target to background ratio in images as non-bound antibody can be cleared from circulation more quickly[13,14]. Smaller fragments also allow better tumor infiltration, which is needed to investigate MDSC locations[14]. Another benefit of using antibody fragments is that removal of the Fc region of the antibody results in lowered chance of binding to non-target cells and lowers the chance of complement activation upon probe injection. The Fab fragment is the easiest to fabricate of these as it can be cleaved from the Fc region with papain.

This project has two main goals: to fabricate a probe and to perform initial feasibility testing *in vivo.* Here we propose an imaging probe using a Fab antibody fragment from the 1A8 Ly6G antibody with conjugated Alexa-Fluor 700. The Fab fragment was chosen because its size of 50 kDa allows for renal clearance while maintaining a higher half-life than other fragments[13,14]. This means that any non-conjugated probe will clear the blood faster than a larger fragment, allowing for a better signal to noise ratio upon imaging. The Fab fragment provides an advantage over other fragments due to its relative ease of fabrication, which is important for a probe that may be used frequently. The fluorophore was chosen to be within the excitation/emission spectrum required to both infiltrate the tissue and avoid tissue damage. Deep red fluorophores are best for this application[15,16]. The Alexa Fluor 700 was chosen because it fits these constraints and also because it has a small size that is ideal for keeping the probe small.

This probe can be evaluated by first fabricating the probe and confirming that the correct fragment types have been generated. The fluorophore efficacy *in vivo* can be evaluated using an off the shelf Ly6G antibody with the Alexa Fluor 700 conjugated.

In this study, we demonstrate the successful generation of a cell line for *in vitro* testing of the probe design. We also demonstrate the generation of Fab fragments with inconclusive results as to the purification of these fragments. We also demonstrate the *in vivo* use of an Alexa Fluor 700 labeled Ly6G antibody.

Results

Cell Line Selection and Nucleofection

MH-S, J774A.1, P388D1, and RAW 264.7 cell lines all showed a population of CD11b high but Ly6G low cells (Figure 1).

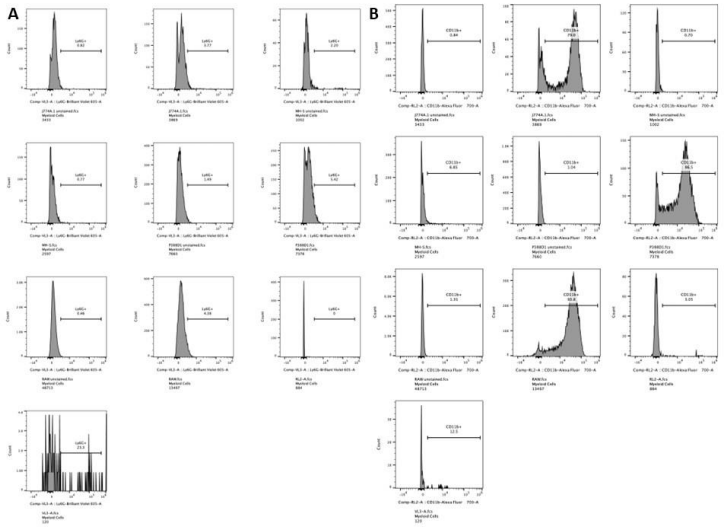

Figure 1: Flow Cytometry on Four Cell Lines. A: Histograms showing expression of Ly6G in unstained and stained for each cell line. Histograms are in the order of unstained then stained for J774A.1; MH-S; P388D1; then RAW. B: Histograms showing expression of Cd11b in unstained and stained for each cell line. Histograms are in the same order as part A.

The lack of an available cell line expressing Ly6G resulted in the need to perform a nucleofection on one of the cell lines. RAW cells grew most quickly out of the four, so this line was selected for nucleofection. Following nucleofection and selection, the control cells not resistant to hygromycin were dead and RAW cells were alive, indicating a successful nucleofection as the hygromycin resistance from the Ly6G plasmid had been transferred into the RAW cells. Flow cytometry was done to confirm that the nucleofection was successful (Figure 2). This data shows that the cell lines did not stain for either CD11b or Ly6G.

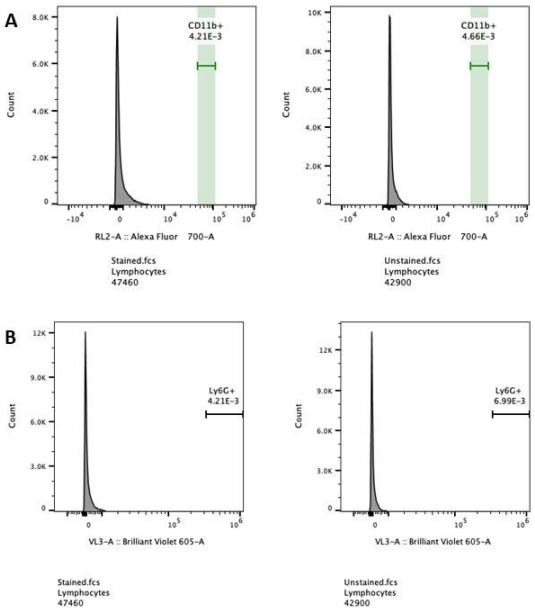

Figure 2: Flow Cytometry of RAW cell line following nucleofection. A: Flow cytometry for CD11b stained and unstained samples. B: Flow cytometry for Ly6G stained then unstained samples.

Fab Fragment Generation

A BCA assay was performed to confirm the presence of protein in each of the samples (Figure 3A).

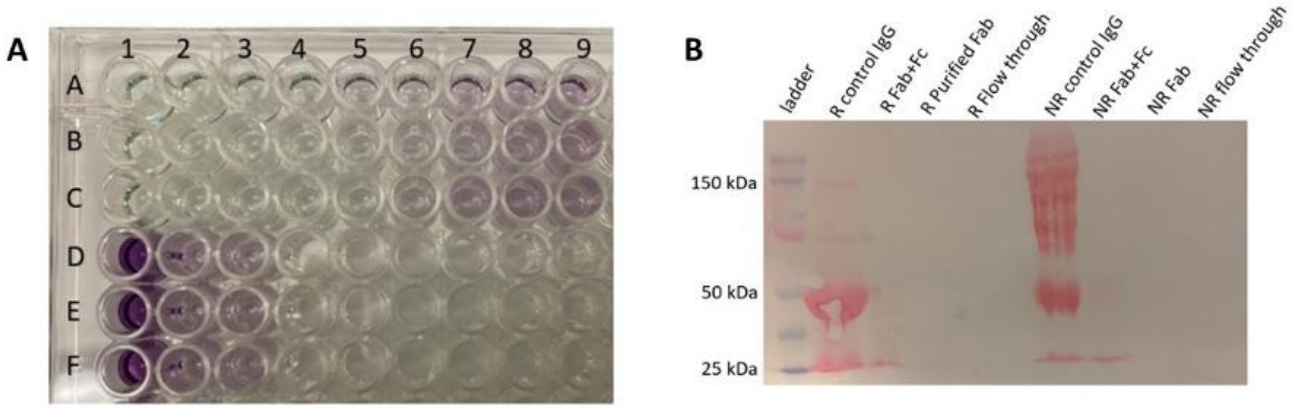

Figure 3: Fab fragment generation evaluation. A: BCA assay showing protein presence and quantification**.** Rows 1-3 are the standards for the assay. Column 1 rows D-F are the unpurified digest of the antibody; column 2 rows D-F are the purified Fab fragments; and column 3 rows D-F are the discard from the Fab purification (should contain Fc fragments).B: Ponceau stained nitrocellulose membrane showing control IgG, unpurified antibody digestion (Fab+Fc), purified Fab fragments, and flow through from purification under reducing (R) and non-reducing (NR) conditions.

This assay showed the presence of protein in the Fab+Fc digest, the purified Fab fragments, and the flow through. The Fab+Fc digest had a high concentration of protein indicated by its deep purple color as compared to the standards. This was not able to be quantified as the protein amount was outside of the range for interpolation. The lower protein concentrations in both the purified Fab and the flow through indicates that some protein had an affinity for the Protein A agarose beads and stayed in the column during purification and some protein was eluted later. Protein A agarose beads have an affinity for Fab fragments but not Fc fragments.

A protein gel was performed to confirm that fragments of the correct size were generated throughout the study (Figure 3B). The gel showed bands at 50 kDa and 25 kDa for the control IgG under reducing conditions, and a smear of protein including more distinct bands at 50 kDa and 25 kDa under non-reducing conditions. The unpurified antibody digestion (Fab+Fc) shows a band at 25 kDa for both reducing and non-reducing conditions. The rest of the samples do not show clear bands.

In vivo pilot study

An in vivo study was performed on mice injected with 4T1 tumors. These mice were injected with an Alexa Fluor 700 Ly6G antibody and imaged (Figure 4).

The images of the mice showed the highest antibody levels at the site of the RO injection at the eye, and then moving down slightly into the mice (Figure 5). All four mice stopped breathing at the 15-minute time point, so this was used as the end point of the experiment. In these 15 minutes, the Alexa Fluor 700 was able to be imaged using the Lago-X imager, which indicates that this fluorophore is a good choice for the imaging. Further experiments can confirm that the Alexa Fluor 700 is a useful tool in imaging within the tumor itself. At this point, organs were harvested to determine if any antibody was able to infiltrate them at low levels. One mouse showed signal in the liver and lungs (Figure 4D).

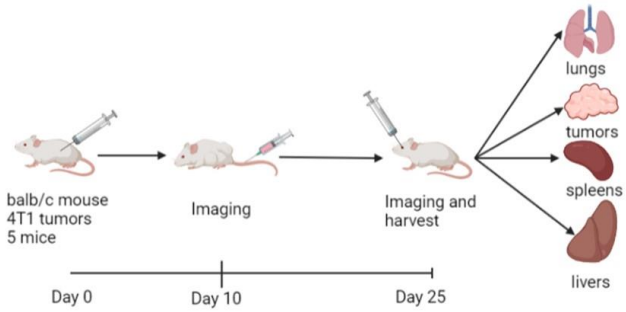

Figure 4: Schematic of mouse experiment. Mice were imaged at the 25-day time point following tumor injection and organs were harvested for further imaging.

Discussion

A Ly6G+ cell line was not confirmed to be able to be generated through nucleofection for future use testing. Selection indicated that Ly6G+ cells had been generated, but flow cytometry was not able to confirm this. The generation of correct antibody fragments were not able to be confirmed by western blotting. The *in vivo* study resulted in the death of all four mice and was not able to demonstrate how the antibody moves throughout the mouse system over time.

Cell Line Selection and Nucleofection

The generation of a Ly6G+ cell line for future experiments is an important step towards *in vitro* evaluation of the probe. Once the probe has been fully fabricated, it can be used in flow cytometry against a

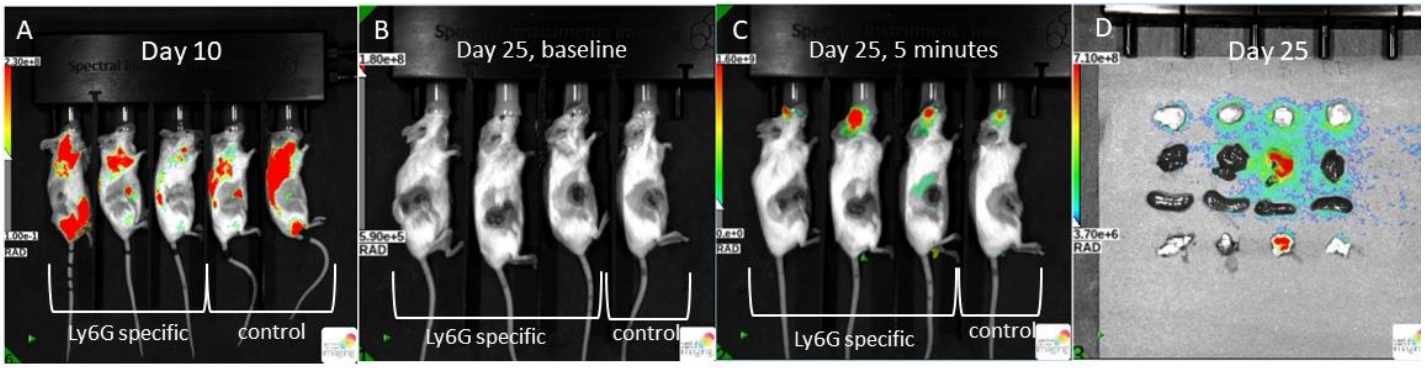

Figure 5: In vivo pilot study with images at different time points. A: Day 10 measurement at 1 hour. B: Day 25 baseline measurement. C: Day 25 measurement 5 minutes post antibody injection. Any fluorescent signal below baseline detection was removed. D: Ex vivo imaging of tumors, livers, spleens, and lungs (top to bottom)

CD11b control flow antibody to determine the specificity of the probe. This sort of experimentation will allow confirmation that the probe did not lose specificity throughout antibody modification or conjugation. Having confidence that the probe maintains its specificity for G-MDSCs following modification will allow for confidence that *in vivo* data is accurately representing MDSC counts.

The results, however, were not able to be confirmed by flow cytometry. The Ly6G plasmid confers resistance to hygromycin, which can be used as a selection agent to kill any non-nucleofected cells in culture. It is also given to control cells nucleofected with a pMAX GFP vector. In the course of culture, the control cells died while the cells nucleofected with Ly6G did not. This indicates initially that the cells were successfully nucleofected. However, the results of flow cytometry show a population of CD11b- and Ly6G- cells. Given that this cell line was CD11b+ in prior flow cytometry experiments, this indicates that there may have been an issue with staining of the Ly6G cells. Going forward, a repeat of the flow cytometry experiment should be completed. One possibility for the experiment showing negative results is that the introduction of Ly6G in the cells could have resulted in conformational changes in CD11b that prevented it from being recognized by flow cytometry antibodies.

One thing to consider in future work with this cell line is that the cell line lost some level of adherence throughout the nucleofection process. Although these floating cells were originally thought to be dead cells, the removal of these cells from culture significantly slowed the cell proliferation and media consumption. Changing the culturing practices of these cells post nucleofection can prevent loss of viable cells. In addition, these cells underwent significant morphology changes following nucleofection. Rather than exhibiting a more spread cell morphology that often clumped into stacks, the cells were much rounder and did not clump as much as before. This indicates issues with cell health. Having a reliable cell line for testing probes is very important for *in vitro* experiments, so optimizing care of these cells post nucleofection is a worthwhile endeavor in the future.

Fab Fragment Generation

The BCA assay shows promising results towards the ability to generate Fab fragments from a full antibody at a small scale. This assay shows that there is protein present in the purified Fab as well as in the flow through, which is to be expected as there should be Fab fragments in the purified digestion and Fc fragments in the flow through. This has to be confirmed via protein gel, however, as these proteins are not necessarily the target proteins. The proteins can be confirmed to be the target proteins through running a protein gel under both reducing and non-reducing conditions. Performing a BCA assay rules out the possibility that there was not protein in the sample if it does not show on the protein stain.

The protein gel should show different results under reducing and non-reducing conditions. This is due to the fact that reducing conditions break down disulfide bonds in proteins while non-reducing conditions do not. Figure 6 shows a schematic of antibody structure, including disulfide bonds in yellow. Under reducing conditions, the full antibody should break down into 25 kDa and 50 kDa proteins. A mixture of papain-cleaved Fab and Fc fragments should break down into all 25 kDa proteins. Fab proteins should likewise show 25 kDa proteins, as will Fc fragments. However, under non-reducing conditions, no disulfide bonds should be broken. This should result in a 150 kDa full protein; 50 kDa Fab fragments; and 50 kDa Fc fragments. The reduced conditions were seen as expected on the gel for the control and Fab+Fc lanes. However, this was not seen for the non-reduced conditions. Although there is a faint band at 50 kDa on the non-reduced Fab+Fc lane, there is also protein in the 25 kDa lane, indicating that some disulfide bonds were broken either in the sample prep or in the Fab fragment digestion process.

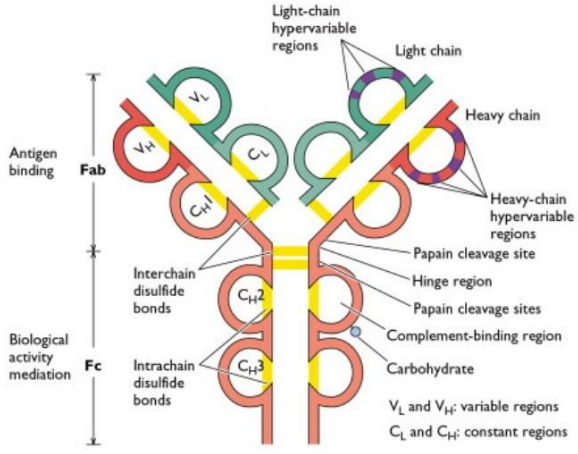

Figure 6: Antibody Molecular Structure. Shows papain cleavage site, binding domains, and disulfide bonds (yellow).[17]

Although some of the lanes showed what was expected, there was no protein visible on the stain for purified Fab or flow through under either reduced or non-reduced conditions. There are several possible reasons for this. The first is that there was not enough protein in the sample to result in a stain. However, as little as 250 ng of protein can be detected in a ponceau stain, so this is likely not the issue given the results of the BCA assay[17]. Another potential factor in this blot is that non-reduced samples tend to run slower than reduced samples and ladders, resulted in larger than expected bands[18]. Although this does not seem to be a large issue in the particular blot shown, it should be considered in any future blots.

In vivo pilot study

This *in vivo* pilot study was designed both as a test of the chosen fluorophore and as an initial look at the kinetics of the Ly6G antibody within the mouse body. The initial study was done to initially look at the antibody at a single time point. The later study was designed to help give an idea of optimum timing of antibody administration. Taking images every five minutes was done to give images of how the antibody is moving over time and was planned to continue out for 45 minutes.

The first study showed high signal in the lung and intestine area. This makes sense as the intestines may have some autofluorescence. In addition, there are likely myeloid cells in the lungs. One mouse died following this study for unknown reasons following recovery from anesthesia.

The 25-day timepoint of the study resulted in all four mice dying within 15 minutes of injection. There are several reasons that this could have happened. The first is that there was an issue with the RO injection itself, which could have resulted in death. Another possibility is that the antibody caused complications in the mouse that resulted in death. This study was initially done at an earlier time point using a tail vein injection, which did not result in complications for the mice. However, one mouse died following this study for unknown reasons, following recovery from anesthesia. This indicates that the antibody in circulation is likely not the primary reason for the mouse death. However, the presence of sodium azide in the antibody could potentially have resulted in complications when injected so closely to the brain. This would explain the acute nature of the mouse death.

The results from the tumor and organ harvest indicate that 15 minutes is not a great enough amount of time to result in tumor or organ infiltration. The presence of signal in one of the mouse's livers likely indicates that the mouse was excreting some antibody, as this mouse also showed a fluorescent signal from its urine throughout the experiment. A follow-up study imaging tumors again at this time point with the same antibody but administering through IV injection could help confirm whether RO injection was the issue with the study.

Limitations

There are several limitations to this work. The first is that the antibody digestion was completed using a control IgG antibody rather than the 1A8 antibody which would be used for the probe generation. This is largely due to the decreased cost of using a control antibody to demonstrate ability to generate antibody fragments. Another limitation is that the antibody used in the *in vivo* studies was a full antibody rather than an antibody fragment. This means that the antibody likely did not achieve tumor infiltration at the same level as an antibody fragment might. An additional limitation of the *in vivo* study is that the mice died at an early time point that did not allow full circulation of the antibody. It also did not allow time for tumor or other organ infiltration.

Conclusions

Although the probe was not able to be fully developed in the scope of this project, the base was set for continued work to develop a fluorescent probe to image MDSCs in vivo. A cell line was identified and nucleofected to express the desired marker Ly6G, which will serve as a useful tool in future experiments. Fab fragments were also generated, although they were not confirmed to be purified from the Fc fragments. In vivo experiments indicates that IV injection is a better route for probe injection, and that time points on the order of 15 minutes are not enough to result in signal within the tumor. The fluorophore Alexa Fluor 700 was able to be detected within the body. With future development, this probe can be a tool for researchers to better understand how MDSCs are interacting with cancer treatments in the tumor.

A first are for future work is completion of probe fabrication and *in vitro* testing. This will allow for confirmation that the probe design is theoretically able to be used for *in vivo* applications. Repeating the *in vivo* pilot study to get images of mice at later time points can also help provide information on the probe design and on the

best dosing and timing for future *in vivo* experiments. Another area to explore in the probe design is half-life extension. This can be completed in several ways, including PEGylation and binding to albumin[19]. These sorts of modifications can help to extend the half-life of antibody fragments in vivo to ensure that the fragments do not degrade in the bloodstream too quickly to be imaged. Loss of the Fc fragment reduces the stability of the antibody molecule, so maintaining stability is important for an *in vivo* application. Half-life extension comes with its own challenges however, including making sure that the probe size remains small enough to meet design constraints.

Another future area for work is developing a method to relate fluorescent intensity counts to cell counts. The Lago-X images give fluorescent intensity measures, but these do not currently have a direct relation to numerical cell counts. Determining a way to relate these fluorescent counts to cell counts will help to produce both cell count and locational data as is the goal of this project.

Materials and Methods

Cell Culture and Flow Cytometry

Initial cell culture was done on four cell lines to determine if they expressed Ly6G. The four lines were J774A.1, P388D1, MH-S, and RAW 264.7. Following expansion, flow cytometry was performed on each cell line using CD11b as the positive control. The cells were stained with BV605 Ly6G antibody and CD11b AF700 antibody. Flow was run on the Attune flow cytometer with forward scatter set at 350; side scatter at 380; the AF700 channel at 397; and the BV605 channel at 451.

Flow cytometry was repeated following nucleofection of the RAW cell line with Ly6G. This was done using the same panel as before.

Transfection and Nucleofection

Transfection was performed using the Invitrogen One Shot Top 10 competent cells protocol[20]. The Ly6G plasmid by Origene was transfected in the bacterial cells. DNA was then extracted a miniprep kit from Qiagen and the associated protocol[21]. A gel was then run to confirm DNA presence in the extraction and the DNA was quantified with the nanodrop spectrophotometer.

This DNA was used to perform nucleofection the RAW 264.7 cell line using the SF cell line 4D nucleofector kit with nucleocuvette strips from Lonza[22]. Three cuvettes were nucleofected with the Ly6G DNA and 3 cuvettes with the pMAX GFP vector. This followed the Amaxa 4D nucleofector protocol for RAW 264.7 cells. The DS-136 program setting was used on the nucleofector. Following nucleofection, cells were transferred to a 96 well plate. The next day cells were placed under selection in DMEM media with hygromycin at 250 ug/ml. Cells were then expanded for flow cytometry.

Fab Fragment Generation and Purification

Fab fragments were generated from the rat IgG2a isotype control antibody from BioXcell. This was done using immobilized papain resin from GoldBio according to the GoldBio protocol[23]. These resulting Fab and Fc fragments were separated using Protein A agarose beads from GoldBio and the associated protocol[24]. Plastic purification columns from Goldbio were used for this protocol.

BCA Assay

BCA assays were performed to confirm the protein concentrations in the Fab +Fc mixture, the purified Fab fragments, and the flow through from the purification. This was performed using the Pierce BCA Protein Assay Kit and associated protocol[25]. However, 2 ul of sample and 100 ul of solution were used for the standards and samples rather than the suggested amounts. The assay was read on the ELx800 universal microplate reader from Bio-tek instruments and analyzed using the KCJunior software.

Protein Gel and Staining

A protein gel was performed on the Emperor Penguin Water Cooled, Dual Gel, Electrophoresis system with an 8% acrylamide gel. Samples were run for the unpurified antibody digestion (Fab+Fc), the purified Fab fragments, and the flow through along with a control IgG antibody. These samples were prepared both under reducing and non-reducing conditions. One lane was left empty in between the reducing and non-reducing samples to prevent diffusion of 2-mercaptoethanol into the non-reducing samples. The Biorad precision plus protein dual standard ladder was used to determine protein sizes. The gel was run at a constant 35 mamp for 50 minutes. The gel was first stained with Coomassie stain for 1 hour then de-stained for 2 hours on the first gel iteration[26]. In future iterations, the gel was transferred onto a nitrocellulose

membrane using the Trans-blot SD Semi-dry transfer cell from Biorad. This membrane was then stained using Ponceau dye for 15 minutes and de-stained using diH20 until the background was clear.

In vivo Imaging

5 balb/c mice were chosen for tumor injection. These mice were anesthetized with a ket/dex mixture then shaved and ear punched. Each mouse was injected subcutaneously with 400,000 4T1 tumor cells suspended in PBS. Mice were initially imaged on Day 10. Two mice were injected with 50 ug of goat anti-mouse IgG (H+L) Cross-adsorbed Secondary Antibody Alexa Fluor 700 in 100 ul PBS. 3 mice were injected with 50 ug Biolegend Alexa Fluor 700 anti-mouse Ly6G antibody straight from the bottle. Following 30 minutes, these mice were anesthetized with isofluorane and imaged in the Lago-X fluorescent reader.

A second imaging set was completed on day 25. One mouse was injected with 50 ug of the control Alexa Fluor 700 antibody, and 3 mice were injected with 50 ug of Ly6G Alexa Fluor 700 Antibody. A baseline image was taken to evaluate background fluorescence. The settings used for imaging were: bin 4; emission wavelength 675; excitation wavelength 730; power 15%; exposure time 3; FOV 20; Fstop 2.0; and object height 1.0. These mice were imaged every five minutes beginning right after injection. Following reading with the whole mouse, mice were euthanized, and their tumors, lungs, spleens, and livers were removed for imaging. This was completed with the same settings as before, but with the object height set at 0.5.

End Matter

Author Contributions and Notes

Acknowledgments

References

1. 1. Marvel, D. & Gabrilovich, D. I. Myeloid-derived suppressor cells in the tumor microenvironment: expect the unexpected. *J. Clin. Invest.* **125**, 3356–3364 (2015).
2. Bronte, V. *et al.* Recommendations for myeloid-derived suppressor cell nomenclature and characterization standards. *Nat. Commun.* **7**, 12150 (2016).
3. Youn, J.-I. & Gabrilovich, D. I. The biology of myeloid-derived suppressor cells: The blessing and the curse of morphological and functional heterogeneity. *Eur. J. Immunol.* **40**, 2969–2975 (2010).
4. Ostrand-Rosenberg, S., Sinha, P., Beury, D. W. & Clements, V. K. Cross-talk between myeloid-derived suppressor cells (MDSC), macrophages, and dendritic cells enhances tumor-induced immune suppression. *Semin. Cancer Biol.* **22**, 275–281 (2012).
5. Umansky, V., Blattner, C., Gebhardt, C. & Utikal, J. The Role of Myeloid-Derived Suppressor Cells (MDSC) in Cancer Progression. *Vaccines* **4**, 36 (2016).
6. Julie A Sterling. Full article: Myeloid-derived suppressor cells expand during breast cancer progression and promote tumor-induced bone destruction. *OncoImmunologgy* **1**, 1484–1494 (2012).
7. Hoffmann, S. H. L. *et al.* Visualization and quantification of in vivo homing kinetics of myeloid-derived suppressor cells in primary and metastatic cancer. *Theranostics* **9**, 5869–5885 (2019).
8. Duerr, J. S. *Immunohistochemistry*. *WormBook: The Online Review of C. elegans Biology [Internet]* (WormBook, 2006).
9. Max Schelker, Sonia Feau, Jinyan Du, & Nav Ranu. Estimation of immune cell content in tumour tissue using single-cell RNA-seq data | Nature Communications. *Nat. Commun.* **8**, (2017).
10. Newton, J. M., Hanoteau, A. & Sikora, A. G. Enrichment and Characterization of the Tumor Immune and Non-immune Microenvironments in Established Subcutaneous Murine Tumors. *J. Vis. Exp. JoVE* 57685 (2018) doi:10.3791/57685.
11. Zhang, Y., Zhang, B., Liu, F., Luo, J. & Bai, J. In vivo tomographic imaging with fluorescence and MRI using tumor-targeted dual-labeled nanoparticles. *Int. J. Nanomedicine* **9**, 33–41 (2013).
12. amersham pharmacia biotech. *Fluorescence Imaging: principles and methods*. (Boston University, 2010).
13. Charles A Janeway, J., Travers, P., Walport, M. & Shlomchik, M. J. The structure of a typical antibody molecule. *Immunobiol. Immune Syst. Health Dis. 5th Ed.* (2001).
14. Bates, A. & Power, C. A. David vs. Goliath: The Structure, Function, and Clinical Prospects of Antibody Fragments. *Antibodies* **8**, 28 (2019).
15. Kobayashi, H., Ogawa, M., Alford, R., Choyke, P. L. & Urano, Y. New Strategies for Fluorescent Probe Design in Medical Diagnostic Imaging. *Chem. Rev.* **110**, 2620–2640 (2010).
16. White, A. G., Gray, B. D., Pak, K. Y. & Smith, B. D. Deep-red fluorescent imaging probe for bacteria. *Bioorg. Med. Chem. Lett.* **22**, 2833–2836 (2012).
17. Ponceau S Solution (ab270042) | Abcam. https://www.abcam.com/ponceau-s-solution-ab270042.html.
18. Kirley, T. L. & Norman, A. B. Unfolding of IgG domains detected by non-reducing SDS-PAGE. *Biochem. Biophys. Res. Commun.* **503**, 944–949 (2018).
19. Nelson, A. L. Antibody fragments. *mAbs* **2**, 77–83 (2010).
20. Invitrogen. One Shot Top10 Chemically Competent E.Coli. (2015).
21. Qiagen. Qiaprep Miniprep Handbook. (2020).
22. Lonza. Amaxa 4D Nucleofector Protocol for RAW 264.7. (2010).
23. GoldBio. Generation of Fab & Fc Fragments from IgG. (2019).
24. GoldBio. Antibody Binding Protocol. (2018).
25. thermoscientific. Pierce BCA Protein Assay Kit. (2020).
26. Coomassie Blue staining. *Cornell Institute of Biotechnology | Cornell University* https://www.biotech.cornell.edu/core-facilities-brc/facilities/proteomics-metabolomics-facility/protocols/coomassie-blue-staining.